JOURNAL OF Applied Polymer SCIENCE

Nanopaper Membranes from Chitin–Protein Composite Nanofibers—Structure and Mechanical Properties

Ngesa Ezekiel Mushi,[1] Nuria Butchosa,[1] Qi Zhou,[2,3] Lars A Berglund[1,3]

[1]Department of Fiber and Polymer Technology, Royal Institute of Technology, Stockholm SE-100 44, Sweden
[2]School of Biotechnology, Royal Institute of Technology, AlbaNova University Centre, Stockholm SE-106 91, Sweden
[3]Wallenberg Wood Science Center, Royal Institute of Technology, Stockholm SE-100 44, Sweden
Correspondence to: L. Berglund (E-mail: blund@kth.se)

ABSTRACT: Chitin nanofibers may be of interest as a component for nanocomposites. Composite nanofibers are therefore isolated from crab shells in order to characterize structure and analyze property potential. The mechanical properties of the porous nanopaper structures are much superior to regenerated chitin membranes. The nanofiber filtration-processing route is much more environmentally friendly than for regenerated chitin. Minerals and extractives are removed using HCl and ethanol, respectively, followed by mild NaOH treatment and mechanical homogenization to maintain chitin–protein structure in the nanofibers produced. Atomic force microscope (AFM) and scanning transmission electron microscope (STEM) reveal the structure of chitin–protein composite nanofibers. The presence of protein is confirmed by colorimetric method. Porous nanopaper membranes are prepared by simple filtration in such a way that different nanofiber volume fractions are obtained: 43%, 52%, 68%, and 78%. Moisture sorption isotherms, structural properties, and mechanical properties of membranes are measured and analyzed. The current material is environmentally friendly, the techniques employed for both individualization and membrane preparation are simple and green, and the results are of interest for development of nanomaterials and biocomposites.
J. Appl. Polym. Sci. **2014**, *131*, 40121.

KEYWORDS: fibers; mechanical properties; membranes; biomaterials; porous materials

Received 5 September 2013; accepted 23 October 2013
DOI: 10.1002/app.40121

INTRODUCTION

Chitin is present in biological nanocomposite in the form of microfibrils, here termed as nanofibers. It is the major load-bearing component in exoskeleton of arthropods, as well as in the cell wall of mushrooms, fungi and molds.[1,2] The Young's modulus of α-chitin crystals has been reported to be 150 GPa,[3] similar to the value for cellulose crystals (134 GPa).[4] The mechanical properties of chitin nanofibers extracted from organisms, and related materials, have not been widely studied. It is relevant not only for the understanding of biological nanocomposite structures but also for the interest of new nanocomposites for packaging or biomedical applications. α-Chitin is the most abundant form of chitin and is extracted commercially from crustacean shells which are available as waste from the seafood industry. The structure of crustacean exoskeletons is hierarchically organized, like in many other biological structures.[5,6] Chitin nanofibers are present in layers twisted in helicoidally manner. The diameter of the chitin nanofibers (microfibrils) is ranging from 2.5 to 4.0 nm.[7] The exoskeleton also consists of protein "binders," pigments or extractives, and stiff inorganic minerals like calcite. The protein content in the exoskeleton of crustaceans is typically 20–25% and the mineral content is ca. 40–50%.[1] Protein and chitin are strongly associated with each other to form what is here termed as chitin–protein composite nanofibers (CPF).

Chitin is of interest in industrial applications because of its chemical stability, favorable mechanical properties and non-toxic, bioabsorbable, biodegradable, and biocompatible characteristics.[2] Chitin membranes or films as well as sutures, filaments, and fibers have been developed from regenerated chitin, and used successfully in laboratory and clinical trials. Some of applications where chitin is used include wound healing, drug delivery, immunotherapy, and antimicrobial materials.[2,8,9]

The mechanical behavior of materials from chitin nanofibers is poorly understood, however, there are studies on materials from modified chitin fibers of microscale diameter. The regenerated fibrous chitin membranes with burst strength of 0.72 Pa at 70% porosity and fibers with microscale diameter was prepared from electrospun fibers.[10] The strength and strain to failure of regenerated chitin membranes are ca. 50 MPa and 7.1%[11] and 38 MPa and 5.7%,[8] respectively. Tensile modulus is around

2 GPa,[11] although the porosity of these regenerated chitin membranes were not reported. Membranes or films from chitin derivatives were reported from chitosan or xanthante. Macroporous acetylated chitosan membranes, with a porosity of 62%, had low tensile strength, ca. 9.2 MPa.[12] Regenerated chitin foams and scaffolds have also been studied.[13] Regenerated chitin is prepared from dissolution of chitin macromolecules in solvents such as dimethyl acetamide in 5% lithium chloride,[14] trichloroacetic acid in methylene chloride,[9] or after derivatization of the side groups.[14] However, the use of strong solvents to make regenerated chitin fibers or membranes is problematic. Strong solvents may result in significant chemical changes or degradation, such as chitin deacetylation, and/or reduced molar mass[8]; more environmentally friendly preparation procedures are therefore of great interest.

Recently, chitin nanofibers have been isolated from crustaceans shells.[15,16] Chitin nanofibers with diameters ranging from ca. 10 to 20 nm was reported previously.[16–18] Resulting films had a tensile modulus and strength of ca. 3 GPa and 44 MPa,[19] although details of these experiments were not reported. Fan, et al.[20] used 33% NaOH at 90°C and obtained deacetylated chitin nanowhiskers. Corresponding films showed a Young's modulus of 5 GPa with a tensile strength of 140 MPa,[15] respectively. The nanowhisker-based films are not considered in the present study, since the focus is on preparation of porous, swirled nanofiber membranes based on CPF. Even though the mechanical properties of chitin nanofiber membranes reported by Ifuku and Saimoto[19] were fairly low, they are much better compared to the fibrous membranes from regenerated chitin nanofibers. The use of composite nanofibers isolated directly from the exoskeleton is interesting in terms of their structure and their property potential. In addition, there is no need for environmentally harmful solvents and the mechanical property potential is superior to those of regenerated chitin membranes. Chemically modified deacetylated chitin nanofibers are pH sensitive due to the amine ($-NH_2$) dominated surface. In contrast, the present CPF are not significantly deacetylated during extraction and most of the native characteristics of the chitin–protein complex are preserved.

The main aim of the present work is to prepare CPF for structural characterization, and then prepare nanopaper membranes. The term "nanopaper" is helpful in that the importance of porosity in the films becomes apparent, analogous to regular paper structures based on wood pulp fibers. Porous nanofibrous nanopaper membranes are interesting alternatives to biomedical applications of regenerated chitin membranes, but may also be considered in packaging film and nanostructured composites applications. Mild conditions have enabled the isolation of composite nanofibers of both chitin and protein in the form they exist in an organism, but which are dominated by the topochemical properties of chitin. The CPF nanopaper membrane is prepared with controlled porosity by combining the cellulose nanofiber techniques used by Henriksson, et al.[21] Mechanical performance and thermal stability are evaluated as a function of porosity.

EXPERIMENTAL

Materials

The crude chitin powder from crab shells was bought from Sigma Aldrich (Germany). Other chemicals as well as solvents were also purchased from Sigma Aldrich and used as received.

Disintegration of Composite Nanofibers from Crude Chitin

Composite nanofibers were isolated from crude chitin powder of crab shells after chemical pretreatment to remove the less bound protein with a method similar to the one developed by Ifuku et al.[16] Chitin powder was treated with a dilute solution of ca. 2*M* HCl, 2*M* NaOH and ethanol to remove minerals, protein, and pigments, respectively. The final yield of composite nanofibers from crude chitin was ca. 73%. Washing was performed to neutrality between each treatment step. The pH of the suspension was adjusted to three using acetic acid in order to electrostatically swell the structure. The suspension was then mechanically treated with a kitchen blender (VITA PREP 3) before passing it through the microfluidizer (M-110EH, Microfluidics). Disintegration was achieved by passing the hydrocolloidal suspension ca. 0.5 wt % five times through 400 and 200 μm chambers at a pressure of 900 bar at room temperature (21°C).

Fourier Transform Infrared Spectroscopy (FT-IR)

FT-IR analyses of the individualized composite nanofibers as well as of the crude chitin powder from crab shell were performed in transmission mode on a FT-IR spectrometer Spectrum 2000 (Perkin Elmer). KBr pellets of crude chitin powder and composite nanofibers were prepared from the freeze-dried powdered material. Scanning was performed 16 times over the wavelength range from 600 to 4000 cm^{-1}.

Intrinsic Viscosity

The intrinsic viscosity [η] was measured in N,N-dimethyl acetamide with 8% lithium chloride (DMAc/8 % LiCl); [η] was obtained from the time recorded to pass through the capillary column (Ubbelhode capillary viscometry) at room temperature (21°C).

Ninihydrin-Hydridantin Protein Test

The residual protein content was determined according to the colorimetric method reported previously with slight modifications.[22] The colloidal suspension containing 0.3 g of nanofibers in 60 mL of 10*M* NaOH was autoclaved for 60 min at 121°C and neutralized in cold bath immediately with 12*M* HCl. The suspension was then filtered using a 0.65 μm pore size filter membrane (DVPP, Millipore). The filtrate and washings were collected and water was added to 200 mL to prepare a sample solution. Next, 0.5 mL of the sample solution was mixed with 5 mL of 0.5*M* acetate buffer at pH 5.2 and 5 mL of ninhydrin–hydridantin solution and incubated in boiling water for 10 min. After rapid cooling, the absorbance was measured at 564 nm using a UV-Vis Spectrophotometer (CARY 50Bio). The reference solution was prepared by using 0.5 mL of deionized water instead of the sample solution. The protein concentration of the sample solution was calculated from a calibration curve using bovine with known concentration ranging from 0.1 to 0.85 mg/mL, thus the protein concentration of the nanofibers can be

calculated by the amount of protein in the sample solution divided by the total weight (0.3 g) of the starting nanofibers.

Atomic Force Microscope (AFM)

Nanoscope IIIa AFM (Veeco Instruments, Santa Barbra) was used to characterize the composite nanofibers. A 20 μL drop of 0.001 wt % nanofiber suspension was cast on a freshly cleaved mica surface and air dried. The mica substrate was attached to a specimen holder and analyzed with tapping mode under ambient air conditions [21°C and 50% relative humidity (RH)]. RTESP silica cantilevers (Veeco) with a spring constant of 40 N m^{-1} and a tip radius of 8 nm were oscillated at their fundamental resonance frequencies that ranged between 200 and 400 kHz.

Field Emission Scanning Electron Microscope (FE-SEM) and Scanning Transmission Electron Microscope (STEM)

The morphology of porous CPF nanopaper membranes from composite nanofibers were characterized by using Field Emission Scanning Electron Microscopy (Hitachi S-4800, Japan). The membranes were conditioned in a desiccator overnight to remove moisture and then sputtered with a thin layer of gold/palladium using Agar HR sputter coater. FE-SEM images were captured at 1.0 kV from secondary electrons. STEM characterization of the composite nanofibers was performed using the FE-SEM (S-4800 Hitachi, Japan) equipped with transmitted electron detector. The composite nanofiber sample was deposited on a carbon coated copper grid and stained with uranyl acetate to elucidate the protein distribution. The STEM images were captured at 30 kV.

Preparation of Porous CPF Nanopaper Membranes

A suspension of ca. 0.07 wt % composite nanofibers was mixed using Ultra Turrax mixer (IKA, D125 Basic) for 10 min to allow uniform dispersion and complete disentanglement of the nanofiber aggregates. The solid weight of dry content was ca. 0.3 g. Thereafter, vacuum filtration was performed using a filter funnel of ca. 7.2 cm in diameter and a 0.65 μm pore size filter membrane (DVPP, Millipore) to obtain a nanopaper hydrogel (wet cake) with about ca. 90% water content. Solvent exchange was performed on the hydrogel immediately. The hydrogel was subjected to solvent exchange in acetone, ethanol, and methanol. The porous CPF nanopaper gels CPF-Wat, Met, Et, Acet were dried in the drying stage of a Rapid Köthen sheet former (Germany) at 70 mbar and 93°C.

Porosity

Porosity of the porous CPF nanopaper membrane was obtained indirectly from ratio of weight to bulk volume. Several pieces of sample such as 4–5 with sizes between 1 and 2 cm, covering the middle part and sides where specimens for mechanical test are taken were weighed. Bulk volume was performed using Mercury Intrusion Porosimetry (Micrometrics). The sample pieces were placed in a penetrometer chamber and loaded. The chamber was air evacuated and thereafter completely filled with mercury at atmospheric pressure (15 psi) and ambient conditions (21°C). The bulk volume was obtained from the difference between volume of the penetrometer (ca. 3.616 cm^3 in this case) with and without the sample and bulk density from weight over volume. Porosity is given from bulk density as shown in eq. (1), where ρ_{sample} stands for the bulk density of the sample and ρ_{chitin} is the density of chitin which is assumed to be 1.425 g/cm^3.[23]

$$\text{Porosity} = 1 - \frac{\rho_{sample}}{\rho_{chitin}} \quad (1)$$

Vapour Sorption Isotherm (VSI)

VSI was performed to established moisture content (MC) of the porous CPF nanopaper membranes under different RH conditions. Membrane samples were dried inside the chamber. RH was increased gradually at 30°C temperature from dry state up to 100% while simultaneously weighing the sample at each saturation point.

Dynamic Thermal Mechanical Analysis (DMTA)

DMTA was carried out using TA Instruments Q800 Model. A nanopaper membrane of ca. 5 mm in width and 10 mm in gauge length was prepared. The membrane sample was conditioned at 40°C overnight to stabilize mechanical properties. It was dynamically heated from 25°C to 300°C at a rate of 3°C/min and a frequency of 1 HZ. The dynamic mechanical properties measured include storage modulus and tan δ.

Tensile Test

Tensile test was performed in uniaxial loading. The width of the sample and gauge length was ca. 5 mm and 40 mm, respectively. The membrane samples were conditioned in 50% RH at room temperature overnight. Tensile test was carried out at a strain rate of 4 mm/min using Universal Tensile Machine (Instron 5944, UK) equipped with a 500 N load cell. Tensile properties measured include Young's modulus, Ultimate tensile strength, tensile strain to failure, and work to fracture, which is defined as the area under the stress–strain curve.

RESULTS AND DISCUSSION

Disintegration of Composite Nanofibers from Crude Chitin

Proteins are present in crustacean exoskeletons either weakly or strongly bound to chitin. Strongly bound protein is difficult to remove as compared to other constituents such as calcium carbonate and pigments, because of its strong association with chitin.[6] It has been shown that chitin forms complexes with proteins through histidyl and aspartyl residues.[24] To preserve chitin structure, mild NaOH pretreatment was performed at 8% concentration. At this concentration, the strong protein–chitin interaction is expected to be maintained. The hydrocolloidal suspension was also subjected to only mild mechanical treatment, and was passed five times through 400 and 200 μm chambers at a pressure of 900 bar using the microfluidizer to avoid excessive disintegration of the chitin–protein fibril structure. Figure 1 presents FT-IR spectra of composite nanofibers in comparison with crude chitin powder from crab shells. The doublet peak over 1660 (near 1658) and 1627 (1624) cm^{-1} absorption bands from amide I and II, respectively, in Figure 1(a) shows strong presence of α-chitin as reported previously.[25] The chitin polymorph from crustaceans, including crab shells, is α-chitin.[23] The corresponding peaks from proteins are masked. However, the presence of protein was semi-quantitatively confirmed by colorimetric method based on a ninyhydrin protein test. The average molar mass of the chitin is important in order

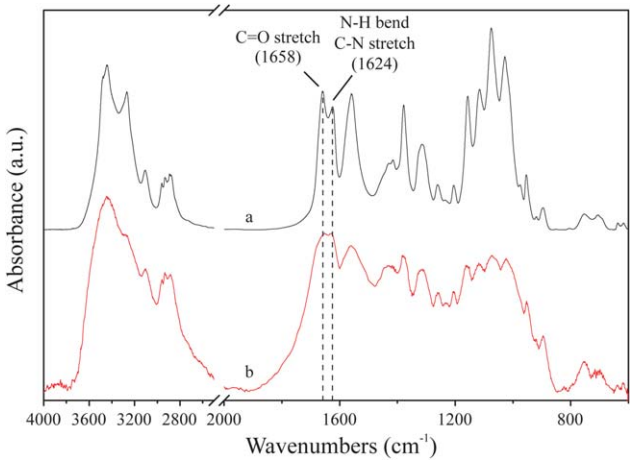

Figure 1. FT-IR spectra of composite nanofibers from crude chitin powder of crab shells, (a) CPF-Wat, and (b) Crude chitin powder from crab shells. [Color figure can be viewed in the online issue, which is available at wileyonlinelibrary.com.]

to estimate degradation effects. The intrinsic viscosity of dissolved composite nanofibers in DMAc/8% LiCl (ca. 40.5 dL/g) is equivalent to an average molecular weight of ca. 1014 kDa according to the Mark-Houwink equation.[26] This compares well with data for chitin from the cuticle of bees after 4% NaOH treatment for 48 hrs. at 80°C.[26] It, thus, seems that the molar mass of chitin was well preserved. Since the chemical pretreatment has limited degradation effects on the chitin, perhaps the absence of a clear protein peak in Figure 1 suggests that most of the residual proteins are present inside the CPF.

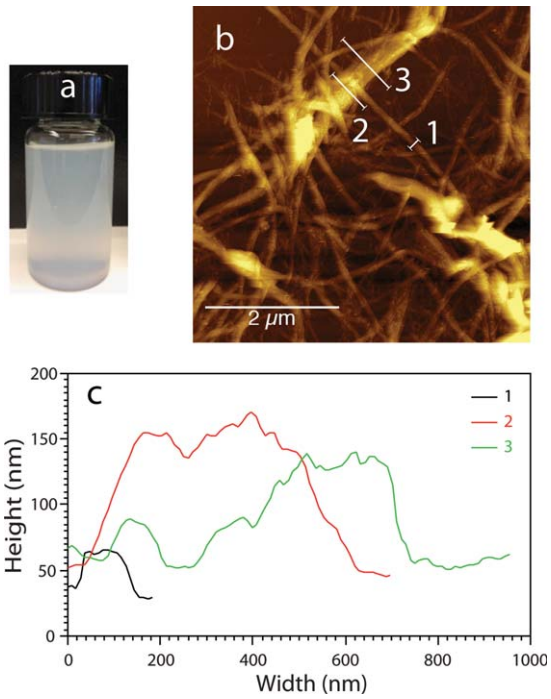

Figure 2. AFM of composite nanofibers on a mica surface: (a) Hydrocolloidal suspension, (b) Height image, and (c) Height profile of the individualised composite nanofiber (legend 1), and individualised composite nanofiber aggregates (legends 2 and 3). The legends refer to specific nanofibers or aggregates in image (b), and the AFM tip is moved perpendicular to the nanofiber or aggregate. [Color figure can be viewed in the online issue, which is available at wileyonlinelibrary.com.]

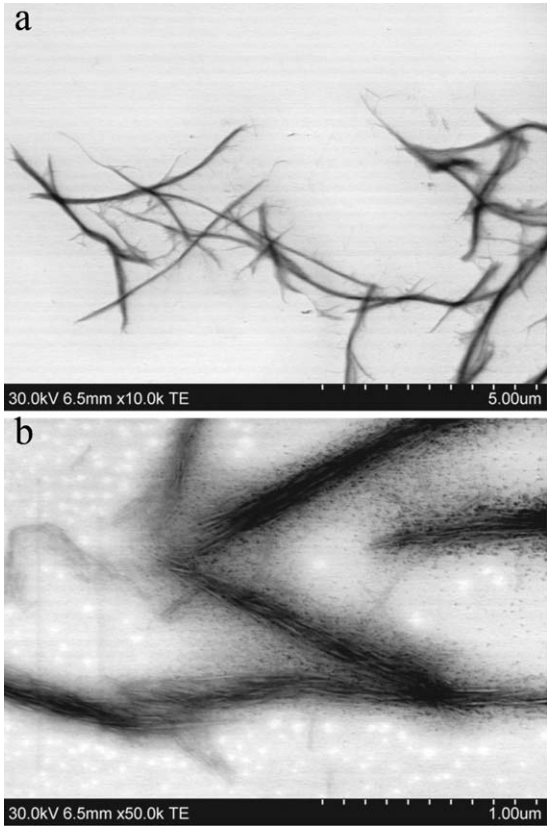

Figure 3. STEM micrographs of composite nanofibers from crude chitin powder of crab shells. Chitin nanocrystals are apparent embedded in the protein matrix at (a) 5 μm and (b) 1 μm scale bar magnification, respectively.

Structure of Composite Nanofibers

The structure of the individualized composite nanofibers is presented in Figures 2 and 3. Figure 2(a) shows the hydrocolloidal suspension of the chitin composite nanofibers. It is a stable colloidal suspension. From the AFM height image, Figure 2(b), a nanofiber length of more than 1 μm is apparent although shorter nanofibers are present as well. The structure of the composite nanofibers may be cylindrical in shape. The diameter of the nanofiber can be estimated from height in Figure 2(c), which shows the height profile of the composite nanofiber (legend 1, profile is perpendicular to axial direction) and composite nanofiber aggregates (legends 2 and 3, profiles in perpendicular directions) in Figure 2(b). The diameter of the composite nanofiber and corresponding aggregates may range from 20 to 30 nm and 70 to 150 nm, respectively. The STEM image in Figure 3(a) complements the structural analysis and gives an impression of nanofiber scale and agglomerate characteristics. There are multiple chitin nanocrystals, apparent as lighter entities inside each nanofiber in the STEM image, see Figure 3(b). They are bonded together by material more difficult penetrated by the electrons, apparent as darker regions.

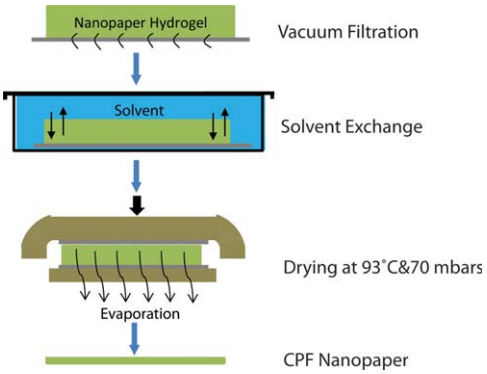

Figure 4. Schematic diagram presentation of solvent exchange and drying procedures akin to paper process. [Color figure can be viewed in the online issue, which is available at wileyonlinelibrary.com.]

These proteins were stained with uranyl acetate. The rod-like geometry of the light chitin indicates that the chitin–protein nanofibers have chitin nanocrystals as building blocks. According to literature, single chitin crystallites have the diameter ranging from 2.5 to 4 nm[6,7] and are 300 nm long.[6] From transmission electron images of the lobster exoskeleton, the size of the chitin–protein-bound nanofibers may approximately be in the order of 50–300 nm in diameter.[6] This supports our data (protein content analysis and Figure 3(b) that the isolated nanofiber structures with larger diameter are actually composite nanofibers of chitin nanocrystals glued together by bound proteins. Thus, it may be concluded that most of the strongly bound protein was retained to chitin with isolation at 8% NaOH. The presence of strongly bound protein to chitin was retained for structural purposes. The strongly bound protein is important for the structural integrity and it can be observed from Figure 2(a) that it is less important for the hydrocolloidal stability. Since the chemical treatments are similar to Ifuku et al.,[16] it is likely that protein is also present in the chitin nanofibers with lateral dimensions of 10–20 nm. Apart from mild NaOH treatment, which removes most of the weakly bound protein, the larger diameter of the present nanofibers is also due to the milder mechanical treatment.

Figure 5. Photographical image of CPF-Wat nanopaper. [Color figure can be viewed in the online issue, which is available at wileyonlinelibrary.com.]

Preparation of Porous CPF Nanopaper Membranes

Porous CPF nanopaper membranes was prepared using the procedure established in our group[21,27] as illustrated in the schematic diagram Figure 4. Figure 5 shows an image of CPF-Wat nanopaper membrane. Composite nanofibers (ca. 0.3 g) were thoroughly mixed in order to achieve a stable hydrocolloidal suspension of uniformly dispersed nanofibers. The hydrocolloid formed a wet cake (or nanopaper hydrogel) of CPF-Wat by filtration in a process similar to hand-sheet fabrication in papermaking.[27]

To create a porous structure, samples designated as CPF-Met, CPF-Et and CPF-Acet were obtained after subjecting the wet cake of CPF-Wat to solvent exchange in methanol, ethanol, and acetone, respectively, followed by drying immediately in a similar fashion.

Structure of Porous CPF Nanopaper Membranes

The structural properties of porous CPF nanopaper membrane such as porosity, thickness, and density are presented in Table I. Porosity of CPF nanopaper without solvent exchange was 22%, but increased to 32, 47, and 58% after solvent exchange in methanol, ethanol, and acetone, respectively, due to the low dielectric constant of the solvents. Water results in the lowest porosity since capillary effects are causing aggregation of nanofibers during evaporation.[28] The specific surface area (SSA) of CPF-Wat was ca. 21.8 m^2/g compared with CPF-Et of ca. 86.6 m^2/g. This indicates that fibril–fibril interaction is reduced because the less hydrophilic solvents hinder secondary bonding interaction and aggregation.

Figure 6 shows the FE-SEM images of porous CPF nanopaper membrane structural characteristics. These images confirm that composite nanofibers form a network structure with individual nanofibers distributed random-in-the-plane in swirled conformation. The porous structure of CPF nanopaper images are in support of density and porosity results as reported in Table I. By comparing Figure 6(b–d) with Figure 6(a), it is apparent that the average pore size is influenced as well. By visual inspection of magnified images, the maximum pore size is estimated to increase from around 150 to 450 nm as porosity increases. Freeze-fractured cross-sections were also studied (see Figure 7). An in-plane layered structure is observed. The nanopaper formed from methanol appears to have a more flat fracture surface although still with a layered structure [Figure 7(a)]. Acetone is a more hydrophobic liquid [Figure 7(b)] and results in a surface with pulled-out layered "flocs" of chitin nanofibers. This may indicate a weaker molecular interaction between the chitin

Table I. Porosity, Density, and Thickness of Porous Chitin Nanopaper Membranes

Nanopaper membrane	Density (g/cm^3)	Porosity (%)	Thickness (μm)
CPF-Wat	1.12	22	42
CPF-Met	0.96	32	51
CPF-Et	0.75	47	53
CPF-Acet	0.61	58	64

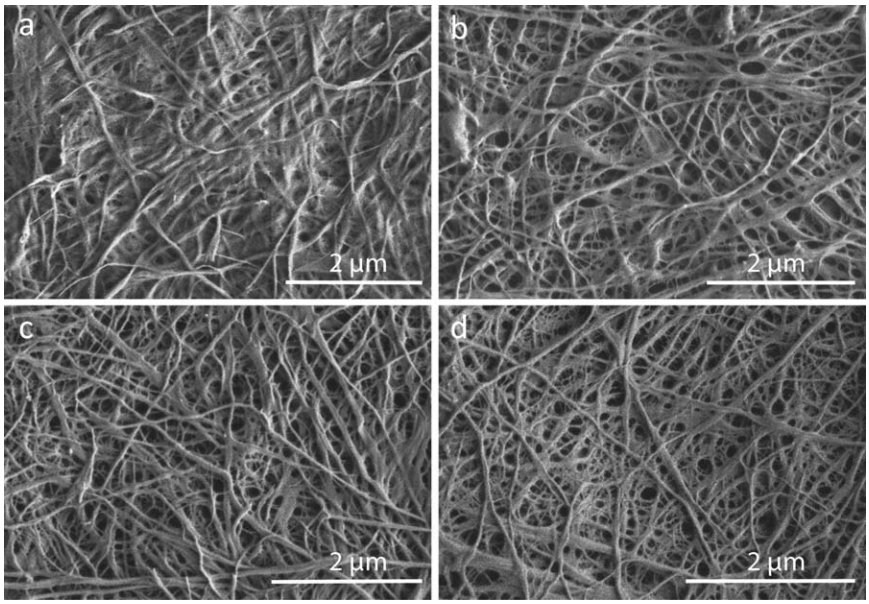

Figure 6. FE-SEM micrographs of porous CPF nanopaper surfaces (a) CPF-Wat (b) CPF-Met (c) CPF-Et (d) CPF-Acet. The scale bars are 2 μm.

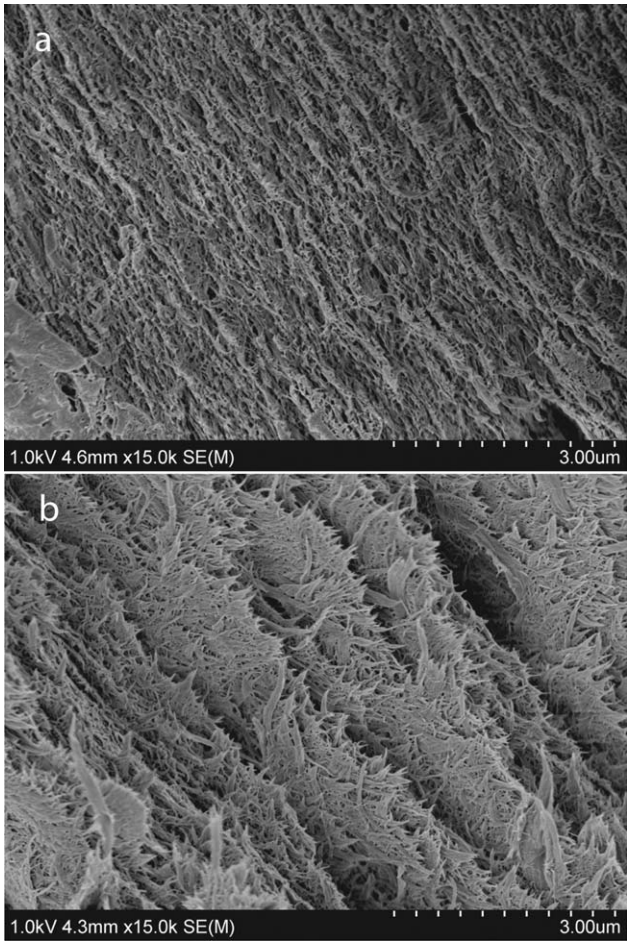

Figure 7. Cross-sectional micrographs showing an in-plane layered structure of the porous CPF nanopaper (a) CPF-Met (b) CPF-Acet. The scale bars are 3 μm.

nanofiber lamellae, due to the nature of the evaporating liquid. Furthermore, the solvent exchanged CPF-Met, CPF-Et and CPF-Acet nanopapers have higher porosity than cellulose nanopaper dried from the same liquids. For example, the maximum porosity of cellulose nanopaper was 40%[21] as compared with 58% for the CPF dried by acetone evaporation. In addition, CPF nanopapers drying from methanol and ethanol resulted in porosities of about 32 and 47%, respectively, which is higher than 28 and 39%, for cellulose nanopaper.

The preparation of porous CPF nanopaper material is very different from most other porous chitin structures, for example, chitin membrane based on microscale diameter fibers prepared from electrospun regenerated chitin fibers,[10] or from regenerated chitin solution i.e. chitin foams or scaffolds prepared by freeze drying[13] or chitin membrane based films by casting.[8,9,14] The pore size in membranes from acetylated chitosan macroporous structures prepared by phase inversion route have been reported in the range from 5 to 18 μm.[12] In the present chitin membranes, mild sodium hydroxide (8%) treatment and mild mechanical disintegration were employed as opposed to strong solvents used for the previous membranes. Simple filtration resulted in submicron pore structures (150–450 nm) and controlled porosity in the range 22–58%. The present membrane is credible for various applications (packaging, tissue scaffolds or selective filtration of inorganic and organic chemicals) suggested for the previous chitin membranes.

MC of Porous CPF Nanopaper Membrane

Figure 8 presents moisture content (MC) against relative humidity (RH) of porous CPF nanopaper. Figure 8 shows that even though the MC increased sharply above 80% RH due to capillary condensation, the maximum MC above 90% RH does not exceed 20%. There is no consistent effect of porosity on MC at 50% RH. The extent of hydration should depend on SSA and the presence of hydrophilic substances, such as proteins. At

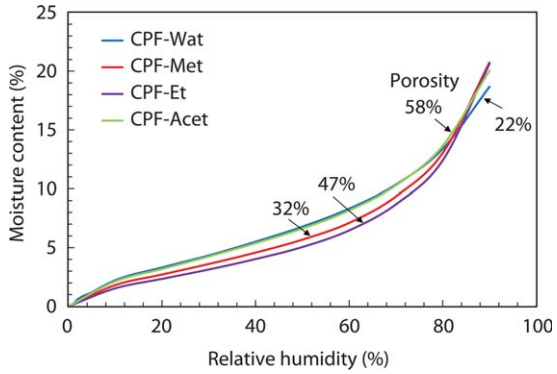

Figure 8. VSI of porous CPF nanopaper membranes with different porosities dried from different liquids (Note: Below 80% RH, the data for 22% porosity overlaps with that at 58% porosity). [Color figure can be viewed in the online issue, which is available at wileyonlinelibrary.com.]

90% RH, the MCs are very different with higher MC at the highest porosity due to capillary condensation effects.

The MC of the CPF nanopaper membranes, are reported in Table II for 50% RH. Data for the present chitin–protein complex are slightly higher than the 3–6% reported in a previous study for chitin[25]; 6% has been reported for cellulose nanopaper[29] and 7% for xyloglucan polymer based films.[30]

Mechanical Properties of the Porous CPF Nanopaper Membrane

Dynamic Mechanical Properties. Figure 9 shows the dynamic mechanical properties of the porous CPF nanopapers. Figure 9(a) is the curve of storage modulus and Figure 9(b) is tan δ against temperature. From Figure 9(a), a shift in storage modulus to lower values is observed as porosity is increased. Data are much higher than for typical glassy polymers. The reason is high intrinsic modulus of chitin nanofibers due to the extended chain conformation of chitin macromolecules. However, storage modulus is maintained over a wide range of temperatures. Simultaneously, two tan δ relaxation regions appear around 150°C and 240°C; see Figure 9(b). There is also a broad relaxation transition between 30°C and 200°C with gradual decrease in storage modulus. Moreover, the tan δ peak temperature between 130°C and 200°C is lowered by about ca. 40°C from 170°C due to lower porosity or the difference in drying liquid. Predominantly, the temperature relaxation between 130°C and 200°C was attributed to the local relaxation of β-1, 4-*N*-acetylglycosamine polymer chain.[31] One may speculate that friction between nanofibers is reduced with increased porosity, and thus the tan δ peak height is reduced. The stable modulus over wide temperature range is of practical importance with respect to thermal stability.

Table II. MC of Porous CPF Nanopaper Membranes at 50% RH

Nanopaper membrane	MC at 50% RH (%)
CPF-Wat	6.8
CPF-Met	6.6
CPF-Et	5.1
CPF-Acet	5.6

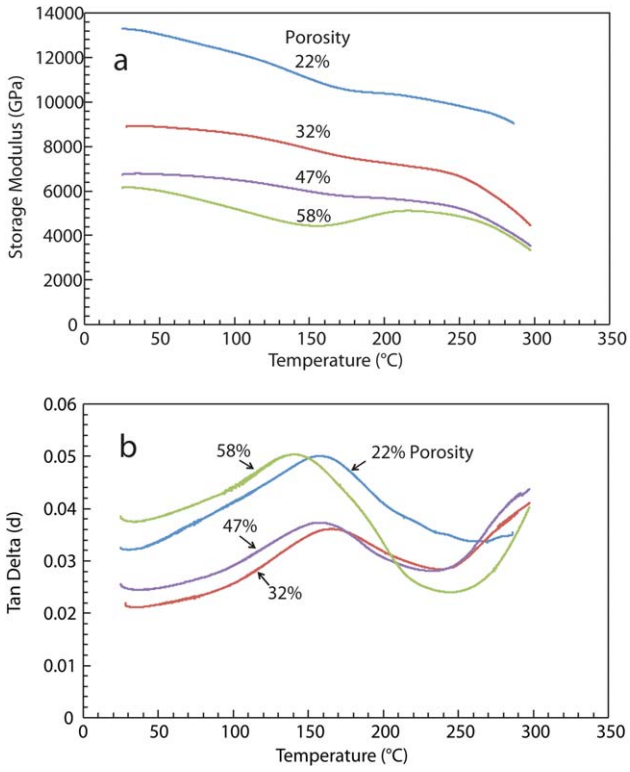

Figure 9. Dynamic thermal mechanical properties of nanopaper membranes with different porosities (see Figure) based on chitin–protein nanofibers, (a) Storage modulus, and (b) Tan δ as a function of temperature. [Color figure can be viewed in the online issue, which is available at wileyonlinelibrary.com.]

Uniaxial Tensile Properties. Figure 10 shows the stress–strain behavior under uniaxial tension. The behavior is non-linear and indicates some limited plasticity, perhaps by nanofiber slippage. The tensile properties are summarized in Table III. The tensile modulus, strength, and strain to failure of CPF nanopaper at 22% porosity are 8.2 GPa, 77 MPa, and 1.4%, respectively. The chitin nanopapers at 22% and 32% porosities are stiff and

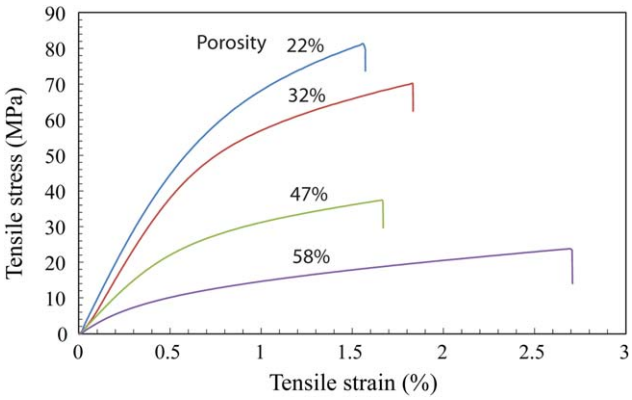

Figure 10. Stress strain curve of CPF nanopaper membranes with varying porosity. [Color figure can be viewed in the online issue, which is available at wileyonlinelibrary.com.]

Table III. Tensile Properties of the CPF Nanopaper Membrane with Varying Porosities (Numbers in Parentheses Are Standard Deviation)

Nanopaper membrane	Porosity (%)	Young's modulus (GPa)	Tensile strength (MPa)	Tensile strain at break (%)	Work to fracture (MJ/m^3)
CPF-Wat	22	8.2 (0.4)	77 (5.6)	1.4 (0.2)	0.77 (0.3)
CPF-Met	32	5.8 (0.2)	48 (4.6)	1.8 (0.2)	0.75 (0.1)
CPF-Et	47	3.3 (0.3)	32 (4.5)	1.3 (0.3)	0.33 (0.1)
CPF-Acet	58	2.5 (0.6)	29 (7.3)	2.7 (0.3)	0.49 (0.2)

strong compared to regenerated chitin membranes. However, they have low tensile strain to failure. The modulus values of ca. 8.2 GPa is similar to the modulus of porous cellulose nanopaper membranes (10–11 GPa). CPF nanopaper membranes show lower strength, strain to failure and work to fracture compared with that of cellulose at 19% porosity.[21] By increasing porosity from 22% to 58%, the modulus and tensile strength were reduced to 2.5 GPa and 29 MPa, respectively, and strain to failure increased to 2.9%. However, tensile properties of CPF nanopaper at 58% porosity appear to be significantly better than for chitin membranes at 70% porosity prepared from electrospun chitin nanofibers.[10] Electrospun fibers from regenerated chitin are expected to be much weaker than the present nanofibers due to lower molecular orientation and probably lower molar mass. Figure 11 compares the relationship between the tensile properties against nanofiber volume fraction. A strong decrease (about 70%) in modulus and strength with nanofiber volume fraction is observed, much stronger than for cellulose nanopaper. One reason may be that the nanofiber interaction (adhesion) is weaker in chitin than in cellulose nanofibers.

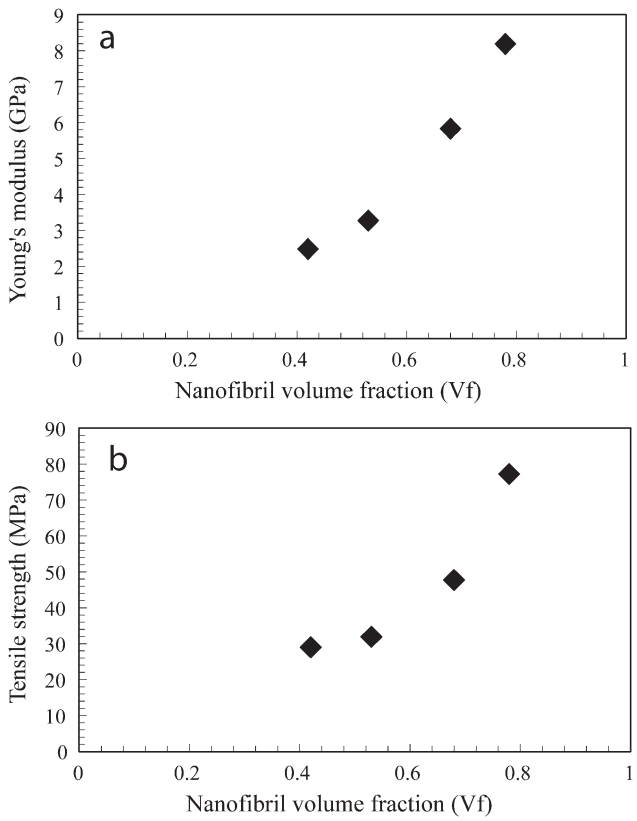

Figure 11. The correlation of nanofiber volume fraction against (a) Young's modulus (b) Tensile strength, and (c) Tensile strain to failure.

The structure of the nanofiber such as size and composition could have significant effect on mechanical properties. Since the preparation route was similar to Ifuku et al.,[16] the structure of the present composite nanofibers may be similar to the nanofibers reported previously.[16–18] However, tensile properties of CPF nanopaper at 22% porosity are high compared to the chitin nanopaper from Ifuku and Saimoto[19] (3 GPa modulus and 44 MPa tensile strength). This indicates that the detailed structure of the individualized chitin nanofibers and their network is very important.

CONCLUSIONS

The potential of chitin nanofibers (rather than the more commonly produced acid-hydrolyzed chitin nanocrystals) from crab exoskeletons was evaluated by nanofiber isolation and preparation of porous nanopaper membranes through a filtration process related to papermaking. The nanofibers that dominate the nanopaper membrane structure are aggregates with typical diameters in the 70–150 nm range. Although FT-IR spectroscopy data suggest that the topochemistry of the nanofiber surfaces was dominated by chitin, it was shown that the nanofibers also contain 7 wt % residual proteins from the crab exoskeleton. This together with STEM images suggests that the nanofiber structure is a composite of chitin nanocrystals bonded together by proteins. Membrane porosities in the range of 22–58% were achieved by drying from various liquids, and pore sizes ranged from 150 to 450 nm. Young's modulus and strength depended strongly on porosity, and were higher than for regenerated chitin membranes from electrospun chitin fibers. Enhanced modulus and strength is expected with reduced porosity, increased nanofiber–nanofiber interaction, and improved intrinsic strength of the nanofibers themselves. Since this material is environmentally friendly and the techniques employed for extraction are simple and green, the results are of interest for further development of environmentally friendly nanomaterial and biocomposites.

ACKNOWLEDGMENTS

Funding from the Carbomat center funded by FORMAS is gratefully acknowledged.

REFERENCES

1. Kurita, K. *Mar. Biotechnol.* **2006**, *8*, 203.
2. Khoushab, F.; Yamabhai, M. *Mar. Drugs.* **2010**, *8*, 1988.
3. Vincent, J. F.; Wegst, U. G. *Arthropod Struct. Dev.* **2004**, *33*, 187.
4. Sakurada, I.; Ito, T.; Nakamae, K. *Makromol. Chem.* **1964**, *75*, 1.
5. Bouligand, Y. *Tissue Cell.* **1972**, *4*, 189.

6. Raabe, D.; Romano, P.; Sachs, C.; Fabritius, H.; Al-Sawalmih, A.; Yi, S.; Servos, G.; Hartwig, H. G. *Mater. Sci. Eng. A.* **2006**, *421*, 143.
7. Blackwell, J.; Weih, M. *J. Mol. Biol.* **1980**, *137*, 49.
8. Aiba, S.; Izume, M.; Minoura, N.; Fujiwara, Y. *Carbohyd. Polym.* **1985**, *5*, 285.
9. Brine, C.; Austin, P. R. Marine Chemistry; ACS Symposium Series: Washington DC, **1975**, p 505.
10. Nishiyama, M.; Kobayashi, Y.; Tokura, S.; Nishi, N. US Pat. 4,392,916, **1983**.
11. Joffe, I.; Hepburn, H. *J. Mater. Sci.* **1973**, *8*, 1751.
12. Zeng, X.; Ruckenstein, E. *Ind. Eng. Chem. Res.* **1996**, *35*, 4169.
13. Chow, K. S.; Khor, E.; Wan, A. C. A. *J. Polym. Res.* **2001**, *8*, 27.
14. Rathke, T. D.; Hudson, S. M. *J. Macromol. Sci. C Pol. R.* **1994**, *34*, 375.
15. Fan, Y.; Fukuzumi, H.; Saito, T.; Isogai, A. *Int. J. Biol. Macromol.* **2012**, *50*, 69.
16. Ifuku, S.; Nogi, M.; Yoshioka, M.; Morimoto, M.; Yano, H.; Saimoto, H. *Carbohydr. Polym.* **2010**, *81*, 134.
17. Ifuku, S.; Nogi, M.; Abe, K.; Yoshioka, M.; Morimoto, M.; Saimoto, H.; Yano, H. *Biomacromolecules* **2009**, *10*, 1584.
18. Ifuku, S.; Nogi, M.; Abe, K.; Yoshioka, M.; Morimoto, M.; Saimoto, H.; Yano, H. *Carbohydr. Polym.* **2011**, *84*, 762.
19. Ifuku, S.; Saimoto, H. *Nanoscale* **2012**, *4*, 3308.
20. Fan, Y. M.; Saito, T.; Isogai, A. *Carbohydr. Polym.* **2010**, *79*, 1046.
21. Henriksson, M.; Berglund, L. A.; Isaksson, P.; Lindstroüm, T.; Nishino, T. *Biomacromolecules* **2008**, *9*, 1579.
22. Shimahara, K.; Takiguchi, Y. *Methods Enzymol.* **1988**, *161*, 417.
23. Carlström, D. *J. Biophys. Biochem. Cytol.* **1957**, *3*, 669.
24. Hackman, R. *Aust. J. Biol. Sci.* **1960**, *13*, 568.
25. Cárdenas, G.; Cabrera, G.; Taboada, E.; Miranda, S. P. *J. Appl. Polym. Sci.* **2004**, *93*, 1876.
26. Draczynski, Z. *J. Appl. Polym. Sci.* **2008**, *109*, 1974.
27. Sehaqui, H.; Liu, A.; Zhou, Q.; Berglund, L. A., *Biomacromolecules* **2010**, *11*, 2195.
28. Fernandes Diniz, J.; Gil, M.; Castro, J. *Wood Sci. Technol.* **2004**, *37*, 489.
29. Svagan, A. J.; Samir, M. A. S. A.; Berglund, L. A. *Biomacromolecules* **2007**, *8*, 2556.
30. Kochumalayil, J.; Sehaqui, H.; Zhou, Q.; Berglund, L. A. *J. Mater. Chem.* **2010**, *20*, 4321.
31. Ogura, K.; Kanamoto, T.; Itoh, M.; Miyashiro, H.; Tanaka, K. *Polym. Bull.* **1980**, *2*, 301.